Main Manuscript for

Polyunsaturated fatty acid structure determines the strength of potentiation of Acid-sensing ion channels

Robert C. Klipp[1] and John R. Bankston[1]

[1] Department of Physiology and Biophysics, University of Colorado Anschutz Medical Campus, Aurora, CO, USA.

*Corresponding Author: John Bankston, Department of Physiology and Biophysics, Research Complex 1 North, University of Colorado Anschutz Medical Campus, Aurora, CO, 80045.
Phone: 303-724-4909

E-mail: john.bankston@cuanschutz.edu

Author Contributions: J.R.B. and R.C.K. designed the experiments. R.C.K. performed the experiments. J.R.B. and R.C.K. analyzed the data. J.R.B. and R.C.K. wrote the manuscript.

Competing Interest Statement: The authors declare no competing interests.

Classification: Biological Sciences - Physiology

Keywords: Acid-sensing ion channels, Polyunsaturated Fatty Acids, Arachidonic Acid, Docosahexaenoic Acid

This PDF file includes:

Main Text
Figures 1 to 5
Tables 1 to 2

Abstract

Acid-sensing ion channels (ASICs) are thought to be endogenous sensors of acidic pain in inflammatory pathways. It has previously been demonstrated that arachidonic acid (AA), a pain and inflammation promoting molecule, potentiates ASICs. However, a mechanistic understanding of how AA regulates ASICs is lacking. Furthermore, little is known regarding modulation by other polyunsaturated fatty acids (PUFAs). Here we show that PUFAs stabilize the open state of the channel by shifting the pH dependence of activation to more alkaline values, increasing max conductance, and slowing channel desensitization. We examine the effects of 35 PUFAs/PUFA derivatives and show that ASICs can be more strongly potentiated by these lipids than was originally seen for AA. In fact, arachidonoyl glycine (AG) can act as a ligand and activate the channel in the absence of acidic pH. We find that the strength of potentiation is critically dependent upon a negatively charged PUFA head group as well as both the length and the number of doubles bonds in the acyl tail. PUFA-induced shifts in the pH dependence of activation could be eliminated upon mutation of a highly conserved, positively charged arginine in the outer segment of TM1 (R64). Combined our results suggest a hypothesis whereby an electrostatic interaction between the charged PUFA head group and the positively charged arginine side chain potentiates ASIC currents by stabilizing the open state of the channel. This work uncovers a novel putative lipid binding site on ASICs and provides the structural basis for future development of compounds targeting ASICs.

Significance Statement

The Acid-sensing ion channels (ASICs) have emerged as potential therapeutic targets for inflammatory pain. Inflammatory mediators like the polyunsaturated fatty acid (PUFA), arachidonic acid (AA), have been shown to potentiate ASICs and partially mediate ASIC-derived pain. However, the mechanistic understanding of AA and other PUFAs interaction with ASICs is lacking. Here, we demonstrate PUFAs stabilize the open state of ASICs, a mechanism that is dependent on both the flexibility of the PUFA tail as well as the charge of the PUFA head group. Further, we uncover a putative PUFA binding site on ASICs governing potentiating. This work provides insights into the molecules regulating ASICs in inflammation, as well as provide a basis for therapeutic targeting of ASIC-derived pain.

Main Text

Introduction

Over 50% of the dry weight of the human brain is lipid with most of that coming from lipids in cellular membranes (1). Docosahexaenoic acid (DHA) and arachidonic acid (AA) are particularly abundant in the brain and other neuronal tissues (2). Reports have shown that DHA may represent 8-18% of the fatty acids in the adult brain and make up an astounding 50-70% of the fatty acids found in the rod outer segment in the retina (3, 4). There are also regional differences in polyunsaturated fatty acid (PUFA) composition within the brain and within the cell types that make up the brain. DHA makes up ~12% of the lipids in astrocytes while only 2% in microglia (5, 6). This variability in the composition of the plasma membrane can have profound effects on the function of membrane proteins in different regions of the brain or in different cell types.

Neurons cannot synthesize many of these essential long chain PUFAs. However, they can incorporate them into their membranes. PUFAs exist in the membrane both as esterified parts of glycerophospholipids that make up the structure of the cell membrane as well as unesterified single carbon-tail lipids. AA is most commonly found esterified at the sn-2 position of glycerophospholipids such as phosphatidylcholine (PC), phosphatidylserine (PS), and phosphatidylinositol (PI) (7). Unesterified PUFAs can result from either synthesis from dietary precursors like linoleic acid or from liberation from glycerophospholipids via enzymes like phospholipase A2 (8).

Given these two pathways, it is not surprising that the composition of PUFAs in the plasma membrane of cells can be impacted by diet. PUFAs are found abundantly in fish oils and a diet high in DHA or its precursor α-linolenic acid has been shown to increase DHA levels in rodent brains (9–12) Conversely, diets deficient in DHA lead to a decrease in total brain DHA with the brain regions that are normally highest in DHA levels, like the hippocampus, most impacted (13, 14). In addition, pathological conditions can impact unesterified PUFA levels likely due to an increase in phospholipase A2 levels. Patients with traumatic brain

injury show significant increase in AA levels in the cerebrospinal fluid compared to patients with no injury (15, 16). In addition, cerebral ischemia is thought to raise AA levels in the affected tissue (17).

The lipid composition of the membrane can significantly impact the function of membrane proteins including ion channels. KCNQ1 and GIRK channels require phosphatidylinositol 4,5-bisphosphate (PIP_2) to function (18, 19) while cholesterol can alter the function of nAChR and TRPV1 channels (20). PUFAs have been demonstrated to alter the function of several ion channels through direct action on the channels themselves. PUFAs have been shown to activate the large-conductance Ca^{2+}- and voltage-gated K^+ (Slo1 BK) channel with a nanomolar EC_{50} (21–23). In addition, the voltage-gated potassium channel $K_V7.1$ can be either potentiated or inhibited by PUFAs and PUFA derivatives depending on the nature of the lipid (24–30).

Previous work has shown that the PUFA arachidonic acid can modulate the function of a family of pH sensing ion channels called the Acid-sensing ion channels (ASICs). ASICs are voltage-insensitive, pH activated channels, widely expressed throughout the body including in neurons in both the central and peripheral nervous system (31). They belong to the ENaC/Degenerin superfamily of ion channels. They have been demonstrated to impact the sensing of pain and inflammation in the peripheral nervous system as well as fear conditioning, ischemic cell death, and synaptic plasticity in the central nervous system (31).

While there is a growing body of literature on the modulation of the ENaC/Degenerin superfamily of ion channels by direct interaction with lipids in the plasma membrane, overall, little is known about the role lipids play in channel function or the mechanisms of modulation of channel function. PIP_2 potentiates ENaC current through a proposed direct interaction yet has no effect on ASICs (32–35). AA potentiates ASIC function likely through a direct action on the channel while direct modulation of ENaC by PUFAs has not been studied (36, 37). AA potentiation of ASICs leads to increased pH-activated currents in DRG neurons as well as increased action potential firing in response to modest acidification of the extracellular space around the neuron (36, 38). This increased excitability led to an increase in cutaneous pain sensing in rat paws. In addition, exudates from human patients with inflamed joints were able to activate ASICs despite having neutral pH (39). These exudates contained several highly abundant lipids including AA and lysophophatidylcholine (LPC). These lipids were sufficient to activate the channel in the absence of acidic pH. These data suggest that lipids may play a critical role in tuning ASICs in pain sensing neurons. Given the vital role of lipids in ion channel function, it is critical to develop a better understanding of the mechanism of lipid modulation of this family of ion channels.

PUFAs are natural nutraceuticals that have the potential to become lead compounds for rational drug design for targeting ion channels and membrane receptors. It has been suggested that dietary supplementation of ω-3 fatty acids can help patients with cystic fibrosis (40). In addition, PUFAs are being designed as a potential treatment for patients with Long QT syndrome type 1 (24, 27, 29, 30). ASICs are potentially interesting targets for the inhibition of pain and the inhibition of cell death in both ischemia and neurodegenerative disorders. Blockade of ASICs with animal venoms has been shown to dramatically reduce pain in a number of pain models (41, 42). Furthermore, blockade of ASICs shows a significant neuroprotective effect in mice subjected to middle cerebral artery occlusion, a model for stroke (43).

For PUFAs to become viable drug candidates, a better mechanistic understanding of their interactions with their target proteins is required. While AA is known to potentiate ASICs, little is known about how PUFAs, more broadly, interact with and modulate this family of channels. The potential interaction sites for these lipids on the channel have not been identified and the structural features of the lipid that lead to regulation are unknown as well. Here we show that arachidonic acid potentiates ASIC currents by stabilizing the open state of the channel. In addition, we show that other naturally occurring PUFAs and PUFA derivatives like DHA and arachidonoyl glycine (AG) are significantly stronger potentiators of ASIC3 than AA. Given this result, we examined the structural components of the lipid to try and understand the critical structural features of the lipid that lead to stronger potentiation of the channel. Finally, we identified a putative binding site for the PUFA head group on the first transmembrane segment of ASICs near the outer leaflet of the membrane. Taken together, these experiments provide the first look at the structural determinants of lipid regulation of ASICs and could form the basis for pharmacological development of PUFAs or new drugs that target a novel druggable site on ASICs for the treatment of pain or ischemic cell death.

Results

PUFAs Stabilize the Open State of ASICs.

Previous work showed that AA increased ASIC currents by shifting the pH dependence of activation to more alkaline pH (36, 38). We first sought to confirm this result. We began by applying 10μM AA to Chinese Hamster Ovary (CHO) cells expressing ASIC3 with a c-terminal cerulean tag and measuring the $pH_{0.5}$ of activation using the whole-cell patch clamp configuration. Figure 1A shows a representative set of currents in the presence and absence of AA. Application of 10μM AA shifted $pH_{0.5}$ by 0.12 pH units, in good agreement with previous results (Fig. 1B) (38). While shifting the pH dependence of activation, 10μM AA had no effect on the pH dependence of desensitization, again in agreement with previous work (Fig. 1B) (38).

The physiologically relevant concentration of AA in the extracellular space of cells is not well known, however, concentration of unesterified PUFA in plasma has been suggested to be in the 10-50μM range (44–46). This concentration can increase to as high as 400μM depending on diet and can also increase in many pathological conditions including inflammation, ischemia, and epilepsy (44, 46–48). Thus, this modest effect of AA at 10μM may represent the lower end of the potentiation of ASICs by AA. In fact, a number of other ion channels have been demonstrated to be potentiated by PUFAs with EC_{50} values significantly higher than 10μM including $K_V7.1$ (DHA EC_{50} = 50μM) and Kv1.5 (AA EC_{50} = 21μM) (26, 49). Measurement of pH dependences in the presence of higher AA concentrations show that significantly larger potentiation of ASIC3 can be achieved at higher concentrations (Fig. 1C). Plotting the shift in $pH_{0.5}$ as a function of AA concentration and fitting to a Hill-type equation yielded an EC_{50} for AA of 9.73μM ± 3.40μM (Fig. 1D).

In addition to a shift in the pH dependence of activation, we also observed an increase in the current magnitude upon addition of AA even at proton concentrations that should render the channel maximally open. We found that 10μM AA increased maximum conductance of the channel (G_{max}) by 1.2-fold (Fig. 1E). Surprisingly, despite 50μM showing an increased shift in the $pH_{0.5}$, there was no additional increase in the G_{max}. Finally, at a maximally activating pH of 5.5 a clear concentration dependent slowing of the rate of desensitization was seen upon addition of AA (Fig. 1F). Taken together, these data suggest that AA potentiates ASIC3 by stabilizing the open state of the channel.

Potentiation of ASIC3 is Stronger for Other PUFAs.

Work on other ion channels has shown that PUFA regulation of channel function can depend on critical structural features of the lipid (21, 29, 30, 50). We looked at a naturally occurring mono- and polyunsaturated FA as well as a PUFA-derivative for their effect on ASIC3 currents: oleic acid (OA) docosahexaenoic acid (DHA) and arachidonoyl glycine (AG). Perfusion of 10μM OA had no effect on ASIC3 currents at any pH, whereas DHA and AG both caused an alkaline shift in the pH dependence of ASIC3 (Fig. 2A). The magnitude of the shift in the pH dependence of activation caused by DHA and AG were ~2.5-3-fold larger than that of AA at the same concentrations. Again, while there was a strong shift in the pH dependence of activation, there was little shift in the pH dependence of desensitization (Fig. 2B). Once again, we observed small increases in ASIC3 currents at pH 5.5 indicating that AG and DHA also increased G_{max} (Fig. 2C). Interestingly, this increased potentiation was similar for all potentiating PUFAs (~1.2 fold), regardless of the magnitude of their relative shifts in activation pH.

Like with AA, both AG and DHA slowed the rate of desensitization (Fig. 2D). At 10μM, AG showed a large, 1.45-fold slowing of the rate of desensitization, while DHA decreased the rate by 1.16-fold, comparable to that observed for AA (Fig. 2D). The slowing became even more pronounced at 50μM, with DHA and AG decreasing the desensitization rate by 1.68-fold and 2.12-fold, respectively (Fig. 2D).

More strongly potentiating PUFAs and PUFA derivatives like AG have the potential to dramatically impact ASIC mediated currents even at more neutral pH. In fact, at 10μM, AG was able to act as a ligand for ASIC3, causing activation of the channel at neutral pH (Fig. 2E). This effect was concentration dependent with 50μM AG able to induce a non-desensitizing ASIC3 current that was, on average, 3% of the peak current (Fig. 2E). This would represent a potentially large sodium leak current through the channel in the presence of AG. Sodium leak can impact both resting membrane potential and excitability of neurons (51). In addition, at slightly more acidic pH, where we still do not see activation of ASIC3, the presence of even 10μM AG was enough to lead to an ASIC3 current at pH 7.1 that shows both a relatively large peak and a large non-desensitizing component (Fig. 2F). These data suggest that this class of lipids can act as non-proton ligands for ASICs.

A Negatively charged Head Group is Critical for ASIC3 Potentiation.

Given that AG and DHA have large effects on ASIC3 currents while OA has no effect and AA has an intermediate effect, it is clear the precise structure of the lipid impacts the potentiation of the channel. Structurally, PUFAs contain a negatively charge carboxylic acid head group and a long non-polar acyl tail. There are a number of PUFA derivatives that vary in their head groups that allow us to probe the contribution that the head group makes to lipid modulation of ASICs. We compared AA to 8 AA-derivatives with differing head groups and identical AA tails [20(5,8,11,14)] (Fig. 3A) (Table 1). These head groups vary in their propensity to ionize: some head groups can readily ionize (glycine) while others do not (methyl ester). In several voltage-gated ion channels a negatively charged head has been critical for potentiation (21, 26, 50). We hypothesize that the charge of the head group is a critical determinant for lipid potentiation of ASICs as well.

Once again, we used measurements of the pH dependence of activation at 10μM as a measure of potentiation (Table 1). Glycine, serine, and alanine head groups all caused a larger alkaline shift in the $pH_{0.5}$ than AA's native carboxyl head group (Fig. 3B). In comparison, all the neutrally charged head groups were either non- or weak potentiators. Methyl ester and ethanolamide showed a trend towards small alkaline shifts in the $pH_{0.5}$, while methyl amide and ethyl ester had no effect on the channel (Fig. 3B). Finally, the two larger head groups showed differing effects. The ethanolamide phosphate head group shifted the $pH_{0.5}$ to a similar degree as the carboxyl group while the taurine had no effect on $pH_{0.5}$ (Fig. 3B). These data are a clear indication that the head group structure had a profound impact on the ability of the lipid to potentiate ASIC3 currents.

Figure 3C shows the $pH_{0.5}$ shifts from figure 3B plotted as a function of calculated pK_a for the different PUFA head group derivatives. The neutrally charged head groups are grouped off the scale of the x-axis, representing either their lack of ionizable atoms (ethyl ester and methyl ester) or a pK_a well outside the range of pH values used in our experiments (ethanolamide and methyl amide). In general, the head groups with lower pK_a tended to have a larger effect on ASIC3 currents. However, both the taurine and ethanolamide phosphate AA-derivatives, despite their low pK_a, either failed to potentiate ASIC3 currents or weakly potentiated the channel. This reduced efficacy may stem from steric clashes between these larger head groups and the binding site on the channel. The reported pK_a values were calculated using MarvinSketch and reflect the pK_a of the head group plus the lipid tail in solution, not in a bilayer. Certainly, the local environment of the lipid will have a profound effect on the pK_a of the lipid in a real cell. Regardless of the actual pK_a of the lipid, these data suggest that head groups that are more likely to harbor a negative charge are more effective at potentiating ASIC3.

To ensure that we were not missing effects due simply to different potencies for the different head groups, we looked at concentration dependent effects of two weakly potentiating head groups: methyl ester and ethanolamide. To do this, we simply switched between pH 8.0 and pH 6.6 and then added an increasing amount of the lipid as indicated in figure 3D. Compared to the carboxyl head group on AA, which showed a clear increase in ASIC3 current with increasing AA concentration, the methyl ester AA-derivative showed no concentration dependent increase in current and the ethanolamide AA-derivative showed a very modest increase in ASIC3 current (Fig. 3D). These results demonstrate that decreased $pH_{0.5}$ activation shifts observed for the neutrally charged head groups are not simply the result of decreased potency.

Dependence upon a negatively charged head group was not limited to PUFAs with the AA tail [20(5,8,11,14)]. Replacing the carboxyl head group of a docosatetraenoic acid [22(4,10,13,16)] that strongly potentiates ASIC3, with methyl ester, eliminated the alkaline shift of the pH dependence of activation (Fig. 3E). Conversely, two PUFAs, linoleic acid [18(9,12)] and OA [18(9)], that did not shift the activation $pH_{0.5}$ of ASIC3, became potentiators upon replacement of the carboxyl head group with a glycine head group (Fig. 3E).

Length and Double Bond Number Contribute to PUFA Impact on ASIC Function.

Next, we sought to determine the role the tail group plays in regulation of ASICs. In general, the tails are often broken down into four properties: length, number of double bonds, ω-number, and position of the double bonds. To understand the structural elements contributing to PUFA modulation of ASICs, we examined a total of 24 PUFAs with identical carboxyl head groups. A full list of PUFAs and effects on ASIC3 are given in Table 1.

We again measured changes in the pH dependence of activation in response to 10μM lipid. Figure 4A shows 23 PUFAs and their respective shifts in the $pH_{0.5}$ of activation which ranged from a 0.32 pH unit alkaline shift all the way to a 0.07 acidic shift. First, the data indicates that tail length likely makes a

significant contribution to the effect of the PUFA. All PUFAs measured with an 18-length acyl chain either fail to modulate, or weakly (<0.1 pH units) potentiate ASIC3 currents, whereas many of the longer, 20 and 22, chain lengths could shift the pH dependence of activation of ASIC3 to a greater extent (>0.26 pH units) (Fig. 4A). This can also be seen in the heat map in figure 4B. The map is ordered in the same manner as figure 4A and the color scale for the heat map is shown in the inset with dark red denoting the strongest alkaline shifts while dark green denotes a small acidic shift. Each column of the heat map represents a single tail characteristic: length, double bond number, single rotatable bonds, and ω-number.

Our data suggests that a minimum of 3 double bonds was necessary for strong potentiation (Fig. 4 A and B). Across the different tail lengths, we showed that PUFAs with 3-6 double bonds are all capable of being strong potentiators of ASIC3. Our data also suggest that the longer the tail length, the more double bonds are needed to make a strongly potentiating PUFA. For the 20-carbon tail PUFAs, the effective PUFAs all have three or four double bonds. Fewer than three double bonds resulted in lipids that inhibited ASIC3 currents. The mono- and polyunsaturated fatty acids eicosenoic acid [20(14)] and eicosadienoic acid [20(11,14)] both caused an 0.07 acidic shift in the $pH_{0.5}$ of activation. Eicosapentaenoic acid [20(5,8,11,14,17)], which has 5 double bonds, was unable to shift the pH dependence of activation of ASIC3. Increasing the tail length by two carbons led to an increase in the number of double bonds needed for potentiation. For 22-carbon tail PUFAs, 4-6 double bonds were necessary for strong potentiation of ASIC3 currents (Fig. 4 A and B).

Together, these data led us to a hypothesis where both length and double bond number were contributing factors to PUFA potentiation of ASIC3. A simple metric that combines these two structural features is the number of single rotatable bonds present in the acyl tail. The number of single bonds increases with tail length and decreases with the number of double bonds present (rotatable bonds = length – double bonds – 2). For PUFAs with 20- or 22-carbon tails this led to the observation that having 14 or 15 single rotatable bonds led to a PUFA that was able to stabilize the open state of the channel. There were two exceptions; dihomo-γ-linolenic acid [20(8,11,14)] had little to no effect on the $pH_{0.5}$ of ASIC3 and docosatetraenoic acid [22(4,10,13,16)], which has 16 single rotatable bonds, was able to strongly potentiate the channel.

To more explicitly test the hypothesis that the number of single rotatable bonds is a critical factor, we compared two PUFAs sharing identical carboxyl head groups, number of and position of double bonds (positions 4,7,10,13,16), but differ in their lengths (19 vs. 22). These PUFAs are therefore different in their number of single rotatable bonds (12 vs. 15). The PUFA with 15 single rotatable bonds strongly potentiated ASIC3 with a $\Delta pH_{0.5} = 0.27$, whereas the PUFA with the 19-carbon tail and only 12 rotatable bonds, had no effect on channel gating with $\Delta pH_{0.5} = 0.01$ (Fig. 4C). This difference was not simply due to a difference in the concentration at which these two PUFAs impact the channel. Increasing concentrations of the 19-carbon tail PUFA failed to elicit a response whereas the 22-carbon tail PUFA showed a concentration dependent increase in current caused by channel activation at pH 6.6 (Fig. 4D). This suggests that both tail length and number of double bonds are critical determinants of PUFA potentiation of ASICs, but neither are sufficient structural features on their own.

There was no specific double bond position that appeared necessary for potentiation across all lipids tested. However, for the 22-carbon tail PUFAs, a double bond at position 4 was present in every strongly potentiating PUFA (Fig. 4A). Docosapentaenoic acid (DPA) with tail [22(7,10,13,16,19)] shows weaker potentiation than DPA with tail [22(4,7,10,13,16)] despite having the same number of double bonds and sharing 4 out of 5 identical double bond positions. Docosatetraenoic acid [22(7,10,13,16)] fails to alter ASIC3 currents despite having all the same double bonds as DPA [22(4,7,10,13,16)] with the exception of the 4-position. This pattern is not maintained for the PUFAs with 20-carbon tails. Having a double bond near the head group at position 5 results in some PUFAs that are effective and others that are not (Fig. 4A). In addition, there are two strong potentiators that do not have a double bond near the head group: eicosatrienoic acid [20(11,14,17)] and eicosatetraenoic acid [20(8,11,14,17)].

Finally, we examined the relationship between ω-number and the functional effect of the lipid. The ω-number refers to the number of carbons away from the methyl end of the tail that the first double bond appears. Previous work has shown that the ω-number correlates with some effects that PUFAs have on other classes of ion channels (29). However, there was no correlation between ω-number and the potentiation of ASIC3 by PUFAs (Fig. 4B).

An Arginine in the Extracellular Domain of ASICs is Critical for PUFA Potentiation.

We next sought to determine the key ASIC residue(s) important in head group interaction or potentiation. Our structural findings demonstrated that a PUFA head group with a low pK_a is a critical determinant in PUFA potentiation. This dependence upon a negatively charged head group has previously been observed to be important for the potentiation of several ion channels, where interaction occurs through interactions with Y, R, or K residues (22, 26, 30, 52, 53). We therefore sought to test whether PUFAs modulate ASICs through similar interactions.

There were more than 10 Y, R, or K residues near the junction of the aqueous phase and the membrane in ASIC3. We did several experiments to narrow down which residues might be involved in PUFA regulation of ASICs. First, we looked at the potentiation of ASIC1a by PUFAs. We rationalized that if ASIC1a is also potentiated, we could limit our search for the binding site to residues shared in the two isoforms. Like with ASIC3, addition of 10μM DHA resulted in an alkaline shift in the pH dependence of activation (Fig. 5A).

To further narrow down the sight of interaction, we designed an experiment to look at whether PUFA interaction with ASICs occurs at the extra or intracellular leaflet of the plasma membrane. We first added AG to the patch pipette and saw no change in current over one minute. Addition of 10μM AG to the extracellular side resulted in an increase in current that was partially reversible upon removal of the extracellular PUFA (Fig. 5B). If PUFA acted intracellularly, we would have expected a blunted or absent effect of extracellular addition of PUFAs, which was not observed. Thus, we concluded that the PUFA likely interacts with a residue on the outer leaflet of the plasma membrane.

Given this, as well as the apparent isoform-independent effects across ASICs, we looked for extracellular, membrane-proximal Y, R, and K residues conserved among ASIC1a, and 3. This yielded 5 candidate residues as possible interaction sites (Fig. 5C and E). Initial substitution of alanine at each of the 5 positions in ASIC3 resulted in non-functional channels in 4 of the 5 mutants (Table 2). We then made alternate mutations at each position that would neutralize the potential interaction with the side chain but still produce functional channels.

We elected to test the effects of DHA on these mutants due to its stronger potentiation of ASIC3, rationalizing that we would more easily be able to see reductions in PUFA effects in these mutants. We found functional mutations in 4 of the 5 positions and measured the effect on the $pH_{0.5}$ caused by the addition of 10μM DHA. A single position, R64Q, eliminated the shift in the activation $pH_{0.5}$ caused by DHA (Fig. 5D). DHA was still able to potentiate the Y67C and Y68W mutants, but the effect was reduced compared to WT potentiation. We attempted to mutate position Y431 to A and C and found that mutations at this position rarely produced currents and when we were able to see currents, they were too small to use in our experiments (Table 2). Mutation of the equivalent position in ASIC1a(Y424) to C and W likewise yielded no currents in all experiments. Looking at the structure of ASIC1a from chicken, R64, Y67, and Y431 (R65, Y68, and Y425 in the chicken), are all less than 10Å from one another (Fig. 5E). We hypothesize that this cluster of amino acids may provide a binding site for the lipid head group. Mutation of the more distal K428, which resides in the β12 strand just above the membrane, to an alanine yielded functional channels that were still fully potentiated by DHA (Fig. 5D). To further confirm that this region of the channel is a critical structural determinant of PUFA potentiation of ASICs, we also mutated R64 in ASIC1a. R64Q in ASIC1a showed a substantially reduced shift in the $pH_{0.5}$ of activation upon application of 10μM DHA compared to WT shift induced by DHA (Fig. 5D).

Discussion

The results of our study provide mechanistic insight into how lipids, specifically PUFAs, modulate the gating of ASICs. We found that PUFAs act by stabilizing the open state of the channel. This leads to an alkaline shift in the $pH_{0.5}$ of activation, a slowing of the rate of desensitization, and an increase in the maximum conductance of the channel. We also found that the previously identified potentiator, AA, was a comparatively weak modulator of ASICs. The highly abundant endogenous PUFAs, DHA, as well as AA-derivatives like AG and AS, were far stronger stabilizers of the open state of the channel. Furthermore, we found that the precise structural properties of the lipid defined how strongly it potentiated ASIC currents. Head groups with lower pK_a values tended to have stronger effect on the channel while neutral head groups were unable to impact currents. The length and number of double bonds present in the acyl tail also both impacted the effect of the PUFA on the channel. Finally, we identified a site on the channel near the extracellular side of the first transmembrane domain that is critical for potentiation.

Our data shows that PUFAs and PUFA derivatives alter several biophysical properties of ASIC3 currents. We measure a shift in the pH dependence of activation that can be greater than a 0.3 pH unit shift even at relatively low concentrations of PUFA. This result is in contrast to results from cerebellar purkinje neurons which suggested that the potentiation of ASICs by AA did not occur via a shift in the activating pH (37). However, our data is consistent with more recent results from two labs that showed that AA likely acts, at least in part, by shifting the pH dependence of activation (36, 38). It is possible that the lipids that make up purkinje cell membranes could differ, or that the ASIC currents in these cells arise from heteromeric ASICs composed of ASIC1a as well as other isoforms. It will be interesting to see if heteromeric ASICs, particularly those that contain ASIC2a or ASIC2b, still respond to PUFAs.

In addition, our data show that PUFAs increase the current even at saturating pH (G_{max}). We found that several PUFA and PUFA derivatives increased G_{max} by ~20%. While previous work did not explicitly suggest that G_{max} was increased by AA, data from multiple papers is consistent with this hypothesis. Smith and colleagues show a ~8% increase in current elicited by pH 5.4 while Allen and Atwell show a ~40% increase in current elicited by pH 6.0 (36, 37). Work on other channels has shown that the functional effects that occur upon PUFA binding are often independent of one another. In the case of the I_{Ks} channel (K_V7.1/KCNE1), the effect on G_{max} and the voltage-dependence of activation seem to arise from different interaction sites (25, 54). Whether this is also true for ASICs remains unknown. Our data showing that increase in G_{max} is the same at both 10 and 50μM AA, despite the shift in the $pH_{0.5}$ increasing over those same two concentrations, suggests that this may also be the case for ASICs. In addition, AG, AA, and DHA show the same magnitude change in G_{max} despite having significantly different effects on the pH dependence of activation. OA, which does not affect the $pH_{0.5}$, also does not affect G_{max}. It is possible that there are independent binding sites for PUFAs on ASICs and that multiple PUFAs bind to the channel to exert the different effects. It is also possible that a single PUFA can make multiple contacts which can exert independent effects on the channel. Answering these questions will be the focus of future studies.

PUFAs also slowed the rate of desensitization for ASIC3. This was not observed in previous work although a trend towards speeding can be seen in the presence of AA in DRG neurons (36). Taken together, these biophysical changes are all consistent with a family of molecules that acts by stabilizing the open state of the channel. Previous work had been entirely focused on AA. We found that other PUFAs and PUFA derivatives were far stronger potentiators of ASICs. DHA, which is highly abundant in the brain, has a stronger effect on both the $pH_{0.5}$ of activation and the rate of desensitization. In fact, another strongly potentiating lipid, AG, was able to act as a ligand, activating the channel even at neutral pH. The naturally occurring AG elicited a non-desensitizing current in cells expressing ASIC3 that at 50μM was 3% of the peak transient current measured at pH 5.5. It is likely that many of the more strongly potentiating PUFAs and PUFA derivatives found in this study all can activate ASICs at pH 7.4, suggesting this class of lipids can act as an endogenous ligand for this family of channels. This is similar to what has been shown for lysophosphatidylcholine, which can activate ASICs in the absence of acidic pH (39). The appearance of a non-desensitizing current likely occurs because of the large shift in the pH dependence of activation coupled with minimal change in the pH dependence of desensitization. This creates the potential for a so-called “window current” which occurs at a position on the pH dependence curve where the channel has some probability to be open without desensitizing.

The potentiation of ASICs by PUFAs appears to be dependent on several structural features of the lipid. PUFA potentiation of ASICs depends on properties of the fatty acid acyl tail. No one property of the tail was able to determine PUFA potency, rather a combination of the length, number of double bonds, and the position of double bonds are likely all contributing factors. First, we found length to be a critical factor, shorter 18-length tails showed weak to no potentiation, while longer 20- and 22-length tails could be either weak or strong potentiators.

Prior study suggested that the number of double bonds in the PUFA tail is important in ASIC potentiation, with more double bonds leading to greater potentiation (36). This hypothesis was based on the comparison of only 3 different lipids (eicosenoic acid, arachidonic acid, eicosapentaenoic acid). Our data suggests that a combination of tail length and number of doubles bonds may be critical for PUFA regulation of ASICs. It is easiest to monitor single rotatable bond numbers in the tail which represent a combination of tail length and double bonds. Interestingly, in both the 20- and 22-length tails, 14- and 15-rotatable bonds in the tail yielded the strongest potentiation of ASIC3 with a few notable exceptions. Docosatetraenoic acid [22(4,10,13,16)], for instance, has 16 single rotatable bonds but still strongly potentiated the channel. It is therefore possible that certain positions or combination of positions in the tail can impact the PUFA regulation of the channel. For 22-length PUFAs, a double bond at position 4 seemed

to be important for strong potentiation of the channel. This may explain why docosatetraenoic acid [22(4,10,13,16)] strongly potentiated ASIC3 currents despite having 16 single rotatable bonds. However, beyond the 4-position near the head group in the 22-length PUFA tails, there did not appear to be any single position that renders a PUFA a strong or weak potentiator of ASICs.

Understanding how double bond number and position impact the tails and their ability to regulate ion channels will require more study. Numerous studies have demonstrated how small changes in the tail can influence the PUFA flexibility, shape, location within the plasma membrane and the molecules it interacts with (55–57). Unfortunately, studies have largely focused on PUFAs that are endogenously abundant, like OA, DHA, EPA and AA and the bulk of the PUFAs used in our study have not been explored. It is possible that PUFAs that successfully potentiates ASICs share critical tail properties like flexibility or shape.

Our data yielded clearer conclusions about the role of the head group in modulating ASICs. AA-derivatives that had head groups with a lower pK_a, tended to have a larger potentiation of channel function. Substitution of a lower pK_a glycine head group onto AA, for example, both slowed the rate of desensitization and shifted the pH dependence of the channel to a greater extent than AA. Strengthening the hypothesis that the charge on the head group is critical for PUFA regulation was our data showing that neutral head groups had minimal effect on ASIC3 currents even at large concentrations.

In addition, mutagenesis of residues that could make electrostatic interactions with the charged head groups of PUFAs uncovered a putative binding site for the head groups of this class of lipids on ASICs. Removal of the positively charged side chain at R64 resulted in a channel that was no longer potentiated by DHA. Mutation of neighboring residues showed a reduction, but not elimination of the PUFA effect. This suggests the possibility that these residues around R64 create a critical binding surface for the lipid head group on the channel. A more distal mutation at K428 did not impact PUFA modulation of the channel. The presence of a relatively constrained binding site could explain why larger negatively charged PUFAs like arachidonoyl taurine failed to potentiate ASIC3 currents. While our mutagenesis is not direct evidence of binding, it does show that this site is critical for PUFA modulation of ASICs. The simplest hypothesis is that it is an interaction site for the negatively charged head group of the PUFAs. Interestingly, the most recent structure of ASIC1a from chicken shows a lipid present between TM1 and TM2 of the same subunit immediately adjacent to our putative binding (58). This structure was solved by isolating ASIC1a from cellular membranes using SMA copolymers which means the lipid present in the structure is an endogenous lipid. It is easy to speculate that the nature of the lipid that is present at this site can have a significant impact on the dynamics of the TM domains and thus the function of the channel.

Interestingly, a recent study looked at mutation of position R64 and showed that the replacement of the arginine with a hydrophobic amino acid led to an alkaline shift in the pH dependence and a slowing of the desensitization rate (59). The structures of ASIC1a from chicken shows that this residue undergoes a movement during gating that changes the network of interactions that it makes. It is possible the PUFA head group works by disrupting interactions made by R64 in the closed or desensitized state, or by stabilizing critical interactions in the open state.

Interaction between a charged head group and residues on transmembrane segments is a common theme for PUFA regulation of ion channels. For the voltage-gated Slo1 BK channel, the negatively charged head group is thought to make an ion-dipole interaction with a tyrosine in the transmembrane domain of the channel (21, 22). The effect of DHA on Slo1 BK was reduced at more acidic pH. Similarly, $K_v7.1$ regulation by PUFAs is also strengthened by head groups with lower pK_a and again this effect is lessened at lower pH (24, 26, 28, 30). Recent work has suggested that the negatively charged head group interacts with an arginine and a lysine residue on the extracellular side of the voltage sensor and pore domain, respectively (54).

The work on these potassium channels has suggested that lower pH results in protonation of the PUFA head group which in turn leads to a decrease in the propensity to form electrostatic interactions with residues on the channel. This might suggest that PUFA binding to ASICs decreases as pH lowers, implying that PUFAs would have a stronger effect on ASICs at more neutral pH. However, binding of DHA to the pH-gated GLIC channel dramatically speeds the rate of desensitization (53). The pH range over which this channel is activated is significantly more acidic than ASICs, yet DHA still modulates the channel at pH 4.5. Moreover, a crystal structure of the channel in the presence of DHA solved at pH 4, showed the carboxyl head group forming a salt bridge with the guanidinium group of an arginine residue near the extracellular side of a transmembrane helix (53). These data suggest that the carboxyl head group was not fully protonated at pH 4 and was still able to form a salt bridge. The physiological pK_a of the head group for these

lipids is largely unknown and may vary dramatically depending on the cellular context. We hypothesize that the head group of our negatively charged PUFAs and PUFA derivatives are still charged at the pH required to activate ASICs, and that these charged head groups interact with the positively charged arginine side chain at position 64. Future work will be required to determine if R64 is the site of binding or if it serves as a coupling position between PUFA binding and the gate.

ASICs have a wide variety of physiological roles in almost every tissue in the body (31). Our data suggest that ASIC function could vary in different cell types, in part, due to differences in the composition of the plasma membrane. Esterified and unesterified PUFA levels can vary substantially from tissue to tissue and cell type to cell type and may provide a mechanism for tuning the sensitivity of the channel to protons (1). It is still a matter of debate what pH ASICs are likely to experience at synapses. Work in retinal bipolar cells has shown that the synapse may acidify by 0.2-0.6 pH units (60). In our experiments, a pH of ~6.5 is required to activate half of the ASIC3 current and a pH of 6.8 (0.6 pH units below resting pH) would activate almost no ASIC3 currents. However, binding of lipids like DHA or AG represent a potential mechanism to shift the pH range over which ASICs function to more physiological pH. In addition, elevation of PUFA levels often accompany pathological conditions like inflammation (8). Lipids that potentiate ASICs like AA as well lysophophatidylcholine (LPC) are both increased during inflammation and can lead to an ASIC-mediated pain (39). It will be interesting to determine if PUFAs share a common mechanism with LPC. It seems more likely, given the shorter tail and larger head group, that LPC modulates ASIC function through a separate site.

Inhibition of ASICs has been shown to be a potential pathway to developing non-narcotic drugs that can treat pain (42, 61, 62). Our data suggest that PUFAs are potential lead compounds for developing new drugs to modulate ASIC activity. Our data showed that two FAs, monounsaturated eicosenoic acid [20(14)] and polyunsaturated eicosadienoic acid [20(11,14)] both inhibited ASIC3 function by shifting the pH dependence of activation in the acidic direction. Moreover, these PUFAs could further inhibit ASIC function by competing off potentiating PUFAs that bind to the channel during pathological conditions like inflammation. The work presented here identified basic principles that govern PUFA modulation of ASICs and identified a novel putative binding site for the development of ligands and drugs that target ASICs.

Materials and Methods

PUFA Nomenclature. For common PUFAs (AA, OA, DHA, etc.) standard abbreviations are used after being defined in the text. Other PUFAs are named using their tail properties in the format of [length(position of double bonds)]. All acyl tail doubles bonds are in the cis configuration for PUFAs and PUFA-derivatives used in this study. Unless otherwise specified, all PUFAs used in this study contain a carboxyl head group. A full list of the PUFAs used in this study with their head groups, tail lengths and position of doubles bonds is given in Table 1.

Materials and Mutagenesis. PUFAs used in this study were purchased through Cayman Chemical. Plasmids for ASIC1a, and ASIC3 each from rat were gifts from David Julius and subcloned into pcDNA3.1. To visualize cell expression, WT, and mutant ASICs a short proline rich linker was used to join mCerulean3 to the C-terminus of the channel. Point mutants used in this study were made using site-directed mutagenesis either in house or through Biozilla services.

Cell Culture and Transfection. Chinese hamster ovary (CHO-K1) cells (ATCC) were cultured in Ham's F12 media with 10% FBS at 37°C in 5% CO2. Cells at ~70% confluency were transfected with indicated ASIC plasmid DNA. Transfection was achieved either via electroporation with a Lonza 4D Nucleofector unit or through chemical means using Mirus TransIT-Transfection Reagent (Mirus) following the manufacturer's protocols. Following transfection, cells were plated on 12-mm glass coverslips coated in poly-L-lysine.

Electrophysiological Recordings. All experiments were performed in the whole-cell patch-clamp configuration 16–48 h after transfection. Borosilicate glass pipettes (Harvard Apparatus) pulled to a resistance of 2–6 MΩ (P-1000; Sutter Instrument) and filled with an internal solution containing (in mM): 20 EGTA, 10 HEPES, 50 CsCl, 10 NaCl, and 60 CsF, pH 7.2. Extracellular solution contained (in mM): 110 NaCl, 5 KCl, 40 NMDG, 10 MES, 10 HEPES, 5 glucose, 10 Trizma base, 2 CaCl2, and 1 MgCl2, and pH was adjusted as desired with HCl or NaOH. An Axopatch 200B amplifier and pCLAMP 10.6 (Axon Instruments) were used to record whole-cell currents. Recordings were performed at a holding potential of

−80 mV with a 5-kHz low-pass filter and sampling at 10 kHz. Rapid perfusion was achieved using a SF-77B Fast-Step perfusion system (Warner Instruments). Fluorescence was visualized on an Olympus IX73 microscope (Olympus) with a CoolLED pE-4000 illumination system (CoolLED).

Experiments in the presence of PUFA were performed under identical conditions as control experiments except solutions contained the indicated concentration of PUFA. Experiments in the presence of PUFA were all performed with at least a 10 min preincubation with PUFA, unless otherwise specified.

To determine the pH dependence of activation we measured a series of sweeps from a holding pH of 8.0 for 7s followed by a 3s activation pulses at indicated pH. Each activation pH was normalized to the maximally activating pH measured at pH 5.5. For pH dependences using rASIC1a, the same protocol was used except the length of the holding pulse was 50s and the activation pulse was 700ms to minimize the contribution of tachyphylaxis. For pH dependences of desensitization, each sweep was performed using a holding pH of 8.0 for 5s followed by a 22s application of the desensitization solution at the indicated pH. The amount of desensitization was determined at the end of each sweep by measuring the current elicited by a 1.5s pulse of pH 6.0 solution. Each current measured at pH 6.0 was then normalized to the maximal current produced by pH 6.0 determined from a desensitization pH of 8.0.

For paired concentration dependences measured at single pH. Controls were measured using a holding pH of 8.0 applied for 90s, followed by 3s application of pH 5.5, followed again by 90s at pH 8.0 and finally 3s application of pH 6.6. Following the control recording, an identical protocol was followed for increasing concentrations of PUFA on the same cell. Currents in the presence of PUFA were then normalized to their respective controls before averages were calculated.

Data and Statistical Analysis. PUFA structures and pK_a determinations for the various PUFA head group derivatives were made using MarvinSketch chemical editing software (ChemAxon). Calculations of pK_a PUFA molecule (head and tail) in the absence of a bilayer at room temperature. Whole-cell patch clamp current recordings were analyzed using Clampfit 10.6 (Axon Instruments). All data are given as means ± SEM. For normalized data in unpaired experiments, the mean of the PUFA measurements were normalized to the mean of the control measurements. In paired experiments, PUFA measurements were normalized to the control for each individual experiment. For pH dependences, reported $pH_{0.5}$ values represent the mean of the $pH_{0.5}$ values for each individual experiment determined by fitting to a hill-type equation in SigmaPlot10.0:

$$I = \frac{1}{1 + 10^{[(pH0.5 - pHx)n]}}$$

Equation 1

where n = hill number and $pH_{0.5}$=half-maximal activating pH.

$$\Delta pH_{0.5} = \frac{\Delta pH_{0.5} max}{[1 + {EC_{50}}/{C}]^n}$$

Equation 2

where n = hill number, EC_{50} = half maximal potentiation, and $\Delta pH_{0.5}$ = shift in the $pH_{0.5}$.

Desensitization time constants (τ) were determined by fitting to a single exponential + constant function.

$$I = e^{\frac{-t}{\tau}} + C$$

Equation 3

For statistical testing, p-values are reported as calculated, except in cases where p-values were <0.0001, where they are reported as such. For measurements of $pH_{0.5}$, an independent sample two-tailed student t-test was used to compare the $pH_{0.5}$ for each PUFA to that of the appropriate control $pH_{0.5}$. For desensitization rates, a paired two-tailed student t test was performed, comparing time constants at each concentration of PUFA to the control time constants for the same cell.

Acknowledgements

This work was supported by the National Eye Institute R00 EY024267 (to J.R.B.) and the National Institute of General Medical Sciences R35 GM137912 (to J.R.B.) as well as funding from T32 HL007822 (to R.C.K.).

References

1. P. C. Calder, Docosahexaenoic Acid. *Ann Nutr Metab* **69 Suppl 1**, 7–21 (2016).

2. J. S. O'Brien, E. L. Sampson, Fatty acid and fatty aldehyde composition of the major brain lipids in normal human gray matter, white matter, and myelin *. *Journal of Lipid Research* **6**, 545–551 (1965).

3. E. R. Skinner, C. Watt, J. A. Besson, P. V. Best, Differences in the fatty acid composition of the grey and white matter of different regions of the brains of patients with Alzheimer's disease and control subjects. *Brain* **116 (Pt 3)**, 717–725 (1993).

4. R. E. Anderson, Lipids of ocular tissues: IV. A comparison of the phospholipids from the retina of six mammalian species. *Experimental Eye Research* **10**, 339–344 (1970).

5. C. Rey, *et al.*, Maternal n-3 polyunsaturated fatty acid dietary supply modulates microglia lipid content in the offspring. *Prostaglandins Leukot Essent Fatty Acids* **133**, 1–7 (2018).

6. J. M. Bourre, *et al.*, Alterations in the fatty acid composition of rat brain cells (neurons, astrocytes, and oligodendrocytes) and of subcellular fractions (myelin and synaptosomes) induced by a diet devoid of n-3 fatty acids. *J Neurochem* **43**, 342–348 (1984).

7. R. F. Irvine, How is the level of free arachidonic acid controlled in mammalian cells? *Biochem J* **204**, 3–16 (1982).

8. A. Wiktorowska-Owczarek, M. Berezińska, J. Z. Nowak, PUFAs: Structures, Metabolism and Functions. *Adv Clin Exp Med* **24**, 931–941 (2015).

9. S. Hiratsuka, K. Koizumi, T. Ooba, H. Yokogoshi, Effects of dietary docosahexaenoic acid connecting phospholipids on the learning ability and fatty acid composition of the brain. *J Nutr Sci Vitaminol (Tokyo)* **55**, 374–380 (2009).

10. C. G. M. de Theije, *et al.*, Dietary long chain n-3 polyunsaturated fatty acids prevent impaired social behaviour and normalize brain dopamine levels in food allergic mice. *Neuropharmacology* **90**, 15–22 (2015).

11. J. Skorve, *et al.*, Fish oil and krill oil differentially modify the liver and brain lipidome when fed to mice. *Lipids Health Dis* **14** (2015).

12. A. P. Kitson, *et al.*, Effect of dietary docosahexaenoic acid (DHA) in phospholipids or triglycerides on brain DHA uptake and accretion. *J Nutr Biochem* **33**, 91–102 (2016).

13. A. Manduca, *et al.*, Amplification of mGlu5-Endocannabinoid Signaling Rescues Behavioral and Synaptic Deficits in a Mouse Model of Adolescent and Adult Dietary Polyunsaturated Fatty Acid Imbalance. *J Neurosci* **37**, 6851–6868 (2017).

14. J.-C. Delpech, *et al.*, Dietary n-3 PUFAs Deficiency Increases Vulnerability to Inflammation-Induced Spatial Memory Impairment. *Neuropsychopharmacology* **40**, 2774–2787 (2015).

15. S. R. Hogan, *et al.*, Discovery of Lipidome Alterations Following Traumatic Brain Injury via High-Resolution Metabolomics. *J Proteome Res* **17**, 2131–2143 (2018).

16. S. E. Farias, K. A. Heidenreich, M. V. Wohlauer, R. C. Murphy, E. E. Moore, Lipid mediators in cerebral spinal fluid of traumatic brain injured patients. *J Trauma* **71**, 1211–1218 (2011).

17. G. Y. Sun, *et al.*, Role of cytosolic phospholipase A2 in oxidative and inflammatory signaling pathways in different cell types in the central nervous system. *Mol Neurobiol* **50**, 6–14 (2014).

18. C. L. Huang, S. Feng, D. W. Hilgemann, Direct activation of inward rectifier potassium channels by PIP2 and its stabilization by Gbetagamma. *Nature* **391**, 803–806 (1998).

19. G. Loussouarn, *et al.*, Phosphatidylinositol-4,5-bisphosphate, PIP2, controls KCNQ1/KCNE1 voltage-gated potassium channels: a functional homology between voltage-gated and inward rectifier K+ channels. *EMBO J* **22**, 5412–5421 (2003).

20. I. Levitan, D. K. Singh, A. Rosenhouse-Dantsker, Cholesterol binding to ion channels. *Front. Physiol.* **5** (2014).

21. Y. Tian, *et al.*, Atomic determinants of BK channel activation by polyunsaturated fatty acids. *Proc Natl Acad Sci U S A* **113**, 13905–13910 (2016).

22. T. Hoshi, R. Xu, S. Hou, S. H. Heinemann, Y. Tian, A point mutation in the human Slo1 channel that impairs its sensitivity to omega-3 docosahexaenoic acid. *J Gen Physiol* **142**, 507–522 (2013).

23. T. Hoshi, Y. Tian, R. Xu, S. H. Heinemann, S. Hou, Mechanism of the modulation of BK potassium channel complexes with different auxiliary subunit compositions by the omega-3 fatty acid DHA. *Proc Natl Acad Sci U S A* **110**, 4822–4827 (2013).

24. B. M. Bohannon, *et al.*, Polyunsaturated fatty acid analogues differentially affect cardiac NaV, CaV, and KV channels through unique mechanisms. *eLife* **9**, e51453 (2020).

25. S. I. Liin, S. Yazdi, R. Ramentol, R. Barro-Soria, H. P. Larsson, Mechanisms Underlying the Dual Effect of Polyunsaturated Fatty Acid Analogs on Kv7.1. *Cell Rep* **24**, 2908–2918 (2018).

26. S. I. Liin, *et al.*, Polyunsaturated fatty acid analogs act antiarrhythmically on the cardiac IKs channel. *Proc Natl Acad Sci U S A* **112**, 5714–5719 (2015).

27. B. M. Bohannon, *et al.*, Polyunsaturated fatty acids produce a range of activators for heterogeneous IKs channel dysfunction. *J Gen Physiol* **152**, e201912396 (2020).

28. J. E. Larsson, H. P. Larsson, S. I. Liin, KCNE1 tunes the sensitivity of KV7.1 to polyunsaturated fatty acids by moving turret residues close to the binding site. *Elife* **7**, e37257 (2018).

29. B. M. Bohannon, M. E. Perez, S. I. Liin, H. P. Larsson, ω-6 and ω-9 polyunsaturated fatty acids with double bonds near the carboxyl head have the highest affinity and largest effects on the cardiac IKs potassium channel. *Acta Physiol (Oxf)* **225**, e13186 (2019).

30. S. I. Liin, J. E. Larsson, R. Barro-Soria, B. H. Bentzen, H. P. Larsson, Fatty acid analogue N-arachidonoyl taurine restores function of IKs channels with diverse long QT mutations. *eLife* **5**, e20272 (2016).

31. E. Boscardin, O. Alijevic, E. Hummler, S. Frateschi, S. Kellenberger, The function and regulation of acid-sensing ion channels (ASICs) and the epithelial Na+ channel (ENaC): IUPHAR Review 19. *Br J Pharmacol* **173**, 2671–2701 (2016).

32. C. R. Archer, B. T. Enslow, C. M. Carver, J. D. Stockand, Phosphatidylinositol 4,5-bisphosphate directly interacts with the β and γ subunits of the sodium channel ENaC. *Journal of Biological Chemistry* **295**, 7958–7969 (2020).

33. G. Yue, B. Malik, G. Yue, D. C. Eaton, Phosphatidylinositol 4,5-Bisphosphate (PIP2) Stimulates Epithelial Sodium Channel Activity in A6 Cells*. *Journal of Biological Chemistry* **277**, 11965–11969 (2002).

34. T. Li, Y. Yang, C. M. Canessa, Impact of Recovery from Desensitization on Acid-sensing Ion Channel-1a (ASIC1a) Current and Response to High Frequency Stimulation. *J Biol Chem* **287**, 40680–40689 (2012).

35. H.-J. Kweon, S.-Y. Yu, D.-I. Kim, B.-C. Suh, Differential Regulation of Proton-Sensitive Ion Channels by Phospholipids: A Comparative Study between ASICs and TRPV1. *PLOS ONE* **10**, e0122014 (2015).

36. E. S. Smith, H. Cadiou, P. A. McNaughton, Arachidonic acid potentiates acid-sensing ion channels in rat sensory neurons by a direct action. *Neuroscience* **145**, 686–698 (2007).

37. N. J. Allen, D. Attwell, Modulation of ASIC channels in rat cerebellar Purkinje neurons by ischaemia-related signals. *J Physiol* **543**, 521–529 (2002).

38. E. Deval, *et al.*, ASIC3, a sensor of acidic and primary inflammatory pain. *EMBO J* **27**, 3047–3055 (2008).

39. S. Marra, *et al.*, Non-acidic activation of pain-related Acid-Sensing Ion Channel 3 by lipids. *EMBO J* **35**, 414–428 (2016).

40. C. Oliver, H. Watson, Omega-3 fatty acids for cystic fibrosis. *Cochrane Database of Systematic Reviews* (2013) https:/doi.org/10.1002/14651858.CD002201.pub4 (June 13, 2021).

41. S. Diochot, *et al.*, Black mamba venom peptides target acid-sensing ion channels to abolish pain. *Nature* **490**, 552–555 (2012).

42. J. Dibas, H. Al-Saad, A. Dibas, Basics on the use of acid-sensing ion channels' inhibitors as therapeutics. *Neural Regen Res* **14**, 395–398 (2019).

43. Z.-G. Xiong, *et al.*, Neuroprotection in Ischemia: Blocking Calcium-Permeable Acid-Sensing Ion Channels. *Cell* **118**, 687–698 (2004).

44. D. D. Fraser, *et al.*, Elevated polyunsaturated fatty acids in blood serum obtained from children on the ketogenic diet. *Neurology* **60**, 1026–1029 (2003).

45. F. Elinder, S. I. Liin, Actions and mechanisms of polyunsaturated fatty acids on voltage-gated ion channels. *Front. Physiol.* **8** (2017).

46. R. A. Siddiqui, K. A. Harvey, G. P. Zaloga, Modulation of enzymatic activities by n-3 polyunsaturated fatty acids to support cardiovascular health. *J Nutr Biochem* **19**, 417–437 (2008).

47. K. Kuriki, *et al.*, Discrepancies in dietary intakes and plasma concentrations of fatty acids according to age among Japanese female dietitians. *Eur J Clin Nutr* **56**, 524–531 (2002).

48. S. Hammarström, *et al.*, Increased concentrations of nonesterified arachidonic acid, 12L-hydroxy-5,8,10,14-eicosatetraenoic acid, prostaglandin E2, and prostaglandin F2alpha in epidermis of psoriasis. *PNAS* **72**, 5130–5134 (1975).

49. E. Honoré, J. Barhanin, B. Attali, F. Lesage, M. Lazdunski, External blockade of the major cardiac delayed-rectifier K channel (Kv1.5) by polyunsaturated fatty acids. *PNAS* **91**, 1937–1941 (1994).

50. S. I. Börjesson, S. Hammarström, F. Elinder, Lipoelectric modification of ion channel voltage gating by polyunsaturated fatty acids. *Biophys J* **95**, 2242–2253 (2008).

51. D. Ren, Sodium Leak Channels in Neuronal Excitability and Rhythmic Behaviors. *Neuron* **72**, 899–911 (2011).

52. S. I. Börjesson, F. Elinder, An electrostatic potassium channel opener targeting the final voltage sensor transition. *Journal of General Physiology* **137**, 563–577 (2011).

53. S. Basak, N. Schmandt, Y. Gicheru, S. Chakrapani, Crystal structure and dynamics of a lipid-induced potential desensitized-state of a pentameric ligand-gated channel. *eLife* (2017) https:/doi.org/10.7554/eLife.23886 (June 14, 2021).

54. S. Yazdi, *et al.*, Identification of PUFA interaction sites on the cardiac potassium channel KCNQ1. *Journal of General Physiology* **153** (2021).

55. S. C. R. Sherratt, R. P. Mason, Eicosapentaenoic acid and docosahexaenoic acid have distinct membrane locations and lipid interactions as determined by X-ray diffraction. *Chem Phys Lipids* **212**, 73–79 (2018).

56. S. E. Feller, K. Gawrisch, A. D. MacKerell, Polyunsaturated Fatty Acids in Lipid Bilayers: Intrinsic and Environmental Contributions to Their Unique Physical Properties. *J. Am. Chem. Soc.* **124**, 318–326 (2002).

57. S. R. Wassall, W. Stillwell, Polyunsaturated fatty acid–cholesterol interactions: Domain formation in membranes. *Biochimica et Biophysica Acta (BBA) - Biomembranes* **1788**, 24–32 (2009).

58. N. Yoder, E. Gouaux, The His-Gly motif of acid-sensing ion channels resides in a reentrant 'loop' implicated in gating and ion selectivity. *eLife* **9**, e56527 (2020).

59. Z. Chen, G. Kuenze, J. Meiler, C. M. Canessa, An arginine residue in the outer segment of hASIC1a TM1 affects both proton affinity and channel desensitization. *J Gen Physiol* **153** (2021).

60. M. J. Palmer, C. Hull, J. Vigh, H. von Gersdorff, Synaptic Cleft Acidification and Modulation of Short-Term Depression by Exocytosed Protons in Retinal Bipolar Cells. *J. Neurosci.* **23**, 11332–11341 (2003).

61. Y. J. Qadri, A. K. Rooj, C. M. Fuller, ENaCs and ASICs as therapeutic targets. *American Journal of Physiology-Cell Physiology* **302**, C943–C965 (2012).

62. A. Ortega-Ramírez, R. Vega, E. Soto, Acid-Sensing Ion Channels as Potential Therapeutic Targets in Neurodegeneration and Neuroinflammation. *Mediators of Inflammation* **2017**, e3728096 (2017).

63. E. F. Pettersen, *et al.*, UCSF Chimera--a visualization system for exploratory research and analysis. *J Comput Chem* **25**, 1605–1612 (2004).

Figures and Tables

Table 1: $pH_{0.5}$ values for ASIC3 activation for each PUFA measured at 10µM.

PUFA Tail	PUFA Head	$pH_{0.5}$	SEM	n	P
Control		6.56	0.01	70	
18(9)	Carboxyl	6.57	0.04	7	0.864
18(6,9,12)	Carboxyl	6.59	0.01	11	0.138
18(6,9,12,15)	Carboxyl	6.62	0.04	6	0.037
18(9,12)	Carboxyl	6.64	0.03	6	0.014
18(9,12,15)	Carboxyl	6.65	0.02	6	0.003
19(4,7,10,13,16)	Carboxyl	6.57	0.02	6	0.680
20(14)	Carboxyl	6.49	0.02	6	0.008
20(11,14)	Carboxyl	6.49	0.01	4	0.033
20(8,11,14)	Carboxyl	6.60	0.01	5	0.247
20(5,8,11,14,17)	Carboxyl	6.62	0.02	11	0.013
20(5,8,11,14)	Carboxyl	6.68	0.01	7	< 0.0001
20(5,8,11)	Carboxyl	6.85	0.04	8	< 0.0001
20(5,11,14)	Carboxyl	6.85	0.02	4	< 0.0001
20(5,8,14)	Carboxyl	6.86	0.04	5	< 0.0001
20(11,14,17)	Carboxyl	6.86	0.03	7	< 0.0001
20(8,11,14,17)	Carboxyl	6.88	0.03	9	< 0.0001
22(13)	Carboxyl	6.54	0.02	6	0.476
22(7,10,13,16)	Carboxyl	6.55	0.02	6	0.715
22(13,16,19)	Carboxyl	6.57	0.01	4	0.728
22(13,16)	Carboxyl	6.58	0.02	6	0.436
22(7,10,13,16,19)	Carboxyl	6.64	0.03	6	0.007
22(4,10,13,16)	Carboxyl	6.83	0.03	5	< 0.0001
22(4,7,10,13,16,19)	Carboxyl	6.83	0.03	5	< 0.0001
22(4,7,10,13,16)	Carboxyl	6.84	0.03	4	< 0.0001
20(5,8,11,14)	Methyl Amide	6.54	0.05	5	0.475
20(5,8,11,14)	Ethyl Ester	6.59	0.01	4	0.350
20(5,8,11,14)	Ethanolamide	6.62	0.04	5	0.056
20(5,8,11,14)	Methyl Ester	6.64	0.03	5	0.019
20(5,8,11,14)	Alanine	6.75	0.02	4	< 0.0001
20(5,8,11,14)	Serine	6.86	0.03	7	< 0.0001
20(5,8,11,14)	Glycine	6.90	0.03	5	< 0.0001
20(5,8,11,14)	Ethanolamide Phosphate	6.67	0.03	6	0.0002
20(5,8,11,14)	Taurine	6.52	0.01	4	0.258
18(9)	Glycine	6.72	0.02	7	< 0.0001
18(9,12)	Glycine	6.89	0.02	5	< 0.0001
22(4,10,13,16)	Methyl Ester	6.64	0.06	5	0.028

Table 2: $pH_{0.5}$ values for ASIC3 and ASIC1a mutants.

Construct	Condition	$pH_{0.5}$	SEM	n	P
ASIC3 WT	Control	6.56	0.01	70	< 0.0001
	10μM DHA	6.83	0.03	5	
ASIC3(R64Q)	Control	6.86	0.03	10	0.81
	10μM DHA	6.85	0.02	7	
ASIC3(Y67C)	Control	6.50	0.04	4	0.009
	10μM DHA	6.64	0.00	4	
ASIC3(Y68W	Control	6.46	0.00	5	0.0004
	10μM DHA	6.57	0.02	4	
ASIC3(K428A)	Control	6.27	0.02	5	0.003
	10μM DHA	6.57	0.03	4	
ASIC1a WT	Control	6.43	0.05	7	0.002
	10μM DHA	6.70	0.02	6	
ASIC1a(R64Q)	Control	6.48	0.03	8	0.08
	10μM DHA	6.58	0.04	8	

Non-functional/poorly expressing mutants

Construct	Observable Currents
ASIC3(R64A)	0/7 cells
ASIC3(Y67,68A)	0/8 cells
ASIC3(Y431A)	2/28 cells
ASIC3(Y431C)	1/17 cells
ASIC1a(Y424C)	0/5 cells
ASIC1a(Y424W)	0/7 cells

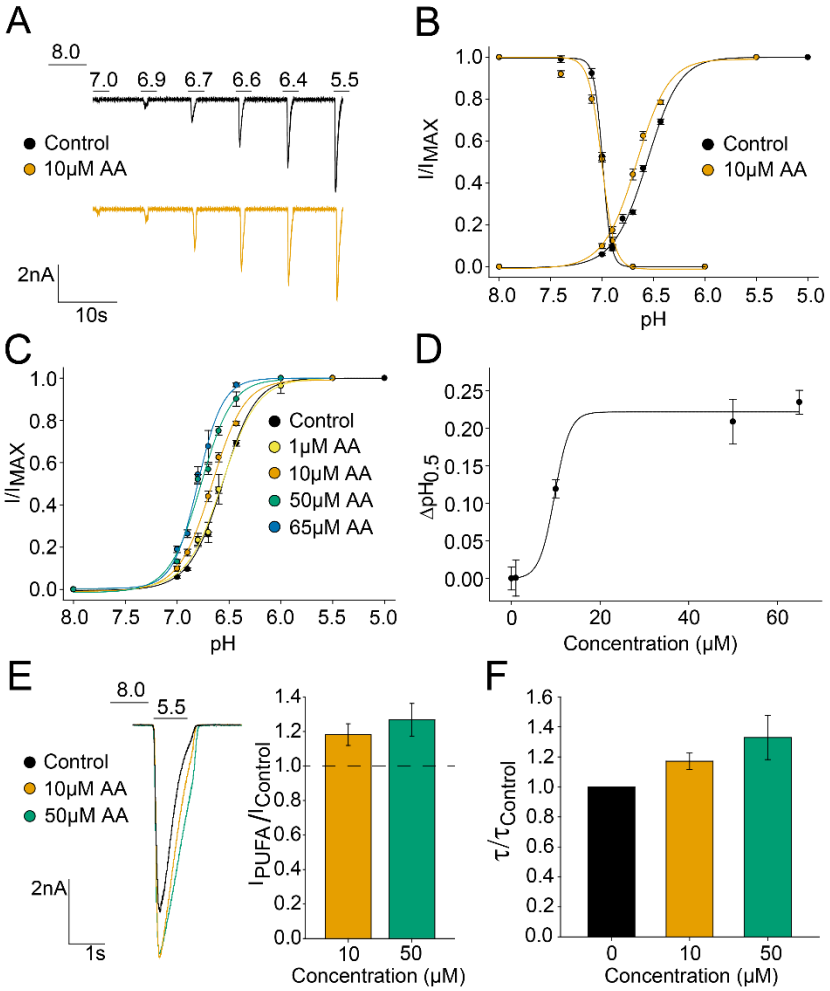

Fig. 1. AA stabilizes the open state of ASIC3. (A) Representative whole-cell recordings showing pH dependent activation of ASIC3 and +/-10μM AA. (B) pH response curves for ASIC3 in control and with application of 10μM AA. Right curves show the pH dependence of activation (Activation $pH_{0.5}$ = 6.68 ± 0.01, n = 7 for AA; and 6.56 ± 0.01, n = 70 for Control; p = 0.00002) while left curves show the pH dependence of desensitization (Desensitization $pH_{0.5}$ = 6.99 ± 0.01, n = 6 for AA; and 7.00 ± 0.01, n = 5 for Control; p = 0.619). (C) Curves showing the pH dependence of activation of ASIC3 at different concentrations of AA (6.56 ± 0.01, n = 70 for Control; $pH_{0.5}$ = 6.57 ± 0.02, n = 5 for 1μM; 6.68 ± 0.01, n = 7 for 10μM; 6.77 ± 0.03, n = 7 for 50μM; 6.80 ± 0.02, n = 6 for 65μM). (D) Activation $pH_{0.5}$ values from data in C plotted as a function of concentration yields a half-maximal activation concentration (EC_{50}) = 9.73μM ± 3.40μM. (E) (left) Representative pH 5.5-evoked currents from a single cell. (right) Bar plot showing the fractional change in the maximum conductance (G_{max}) in response to two concentrations of AA (Fold-increase in G_{max} = 1.18 ± 0.06, n = 10, p = 0.01 for 10μM AA; and 1.27 ± 0.09, n = 10, p = 0.02 for 50μM AA). (F) Bar plot showing the desensitization rate of ASIC3 currents at different concentrations of AA (Fold-increase in time constant (τ) = 1.17 ± 0.05, n = 11, p = 0.02 for 10μM AA; and 1.33 ± 0.15, n = 11, p = 0.0005 for 50μM AA). Time constants were determined by a single exponential fit of currents generated by 3s application of pH 5.5 solution. Each τ_{AA} was normalized to $\tau_{Control}$ for each individual cell prior to averaging. Mean $\tau_{Control}$ = 402.15 ± 16.55, n = 33. All data given as Mean ± SEM.

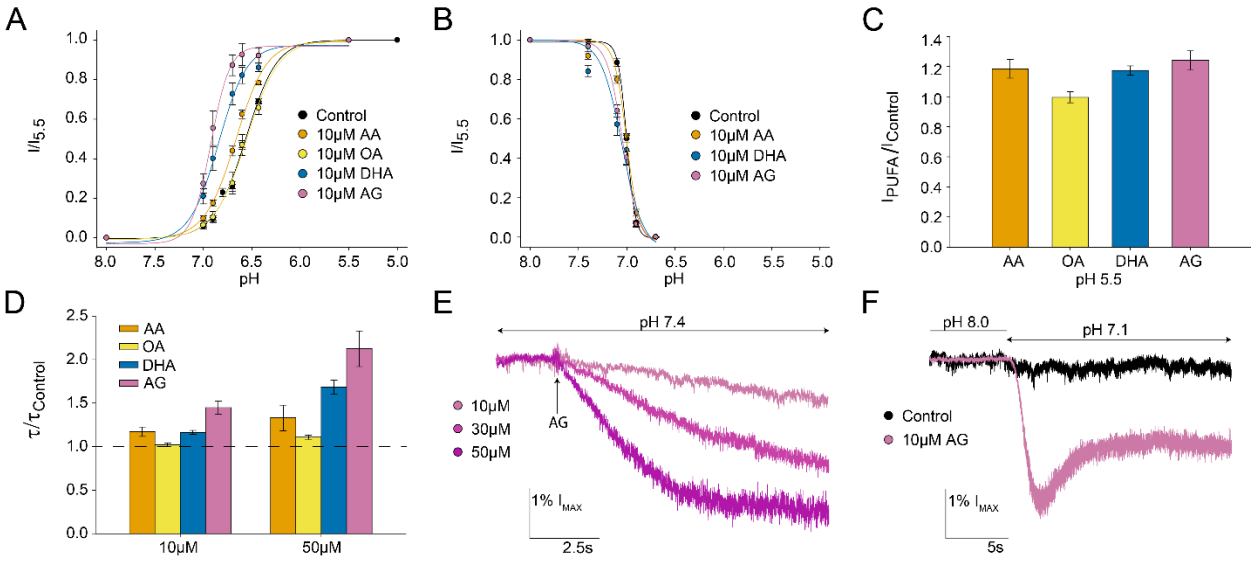

Fig. 2. Other PUFAs and PUFA derivatives more strongly potentiate ASIC3. (A) Curves showing the pH dependence of activation of ASIC3 in the presence of different lipids ($pH_{0.5}$ = 6.57 ± 0.04, n = 7, p = 0.86 for OA; 6.83 ± 0.03, n=5, p < 0.0001 for DHA; and 6.90 ± 0.03, n=5, p < 0.0001 for AG). Control and +10μM AA pH dependences replotted from Fig. 1. (B) Curves showing the pH dependence of desensitization in the presence of different lipids ($pH_{0.5}$ = 7.03 ± 0.05, n=6, p = 0.582 for DHA; and 7.04 ± 0.02, n=5, p = 0.075 for AG). (C) Bar plot showing the fractional change in the maximum conductance (G_{max}) in response to four different lipids concentrations of AA (Fold-increase in G_{max} = 1.04 ± 0.05, n = 4, p = 0.51 for OA; 1.17 ± 0.03, n = 9, p = 0.01 for DHA; and 1.24 ± 0.06, n = 10, p = 0.006 for AG). AA replotted from Fig. 1 for comparison. (D) Bar plot showing the desensitization rate of ASIC3 currents with different lipids at two concentrations AA (Fold-increase in τ = 1.02 ± 0.02, n = 4, p = 0.33 for 10μM OA; 1.11 ± 0.02, n = 4, p = 0.025 for 50μM OA; 1.16 ± 0.02, n = 9, p = 0.0002 for 10μM DHA; 1.68 ± 0.08, n = 9, p < 0.0001 for 50μM DHA; 1.45± 0.07, n = 9, p = 0.0005 for 10μM AG; and 2.12 ± 0.21, n = 4, p = 0.0048 for 50μM AG). Time constants were determined by a single exponential fit of currents generated by 3s application of pH 5.5 solution. Each τ_{PUFA} was normalized to $\tau_{Control}$ for each individual cell prior to averaging. Mean $\tau_{Control}$ = 402.15 ± 16.55, n = 33. (E) Representative ASIC3 currents evoked by application of AG at pH 7.4. (F) Representative ASIC3 currents evoked by application of AG at pH 7.1. All data given as Mean ± SEM.

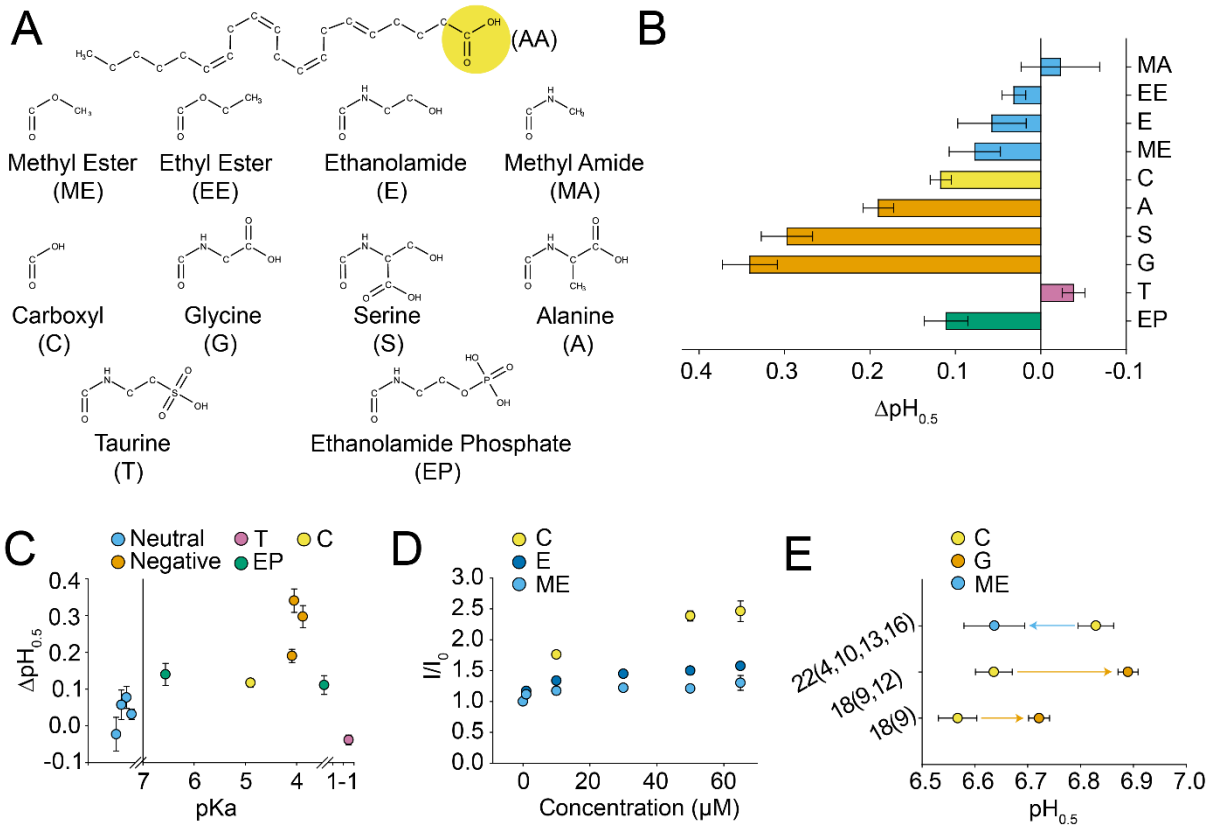

Fig. 3. A negatively charged PUFA head group is critical for potentiation of ASIC3. (A) Structures of AA (top) and the various head groups (below) used to replace AA's native carboxyl head group, creating AA-derivatives used in B-D. (B) Magnitude of shifts ($\Delta pH_{0.5}$) in ASIC3 pH dependence of activation induced by 10μM of the various AA head group derivatives from panel A (Values and statistics given in Table 1). (C) $\Delta pH_{0.5}$ values from B plotted as a function of the of calculated pK_a for the AA-derivatives. AA-derivative with EP head group is plotted twice, reflecting its 2 pK_a values. Neutrally charged head groups (light blue) are plotted to the left of the break in x-axis (at pKa=7) representing that they either are permanently neutral, or the pK_a is sufficiently large that head groups remain neutral at all pH values tested. (D) Plot showing the fractional change in peak current for three different lipids at increasing lipid concentrations. Currents were measured from pH jumps from 8.0 to 6.6 and peak currents at each concentration were normalized to peaks in the absence of PUFA. (E) Plot showing the $pH_{0.5}$ of 3 pairs of lipids. Tail length and double bond position is indicated on the y-axis. Head group is indicated in the key. Arrows denote the shift from the carboxyl head group to the substituted head group. All data given as Mean ± SEM.

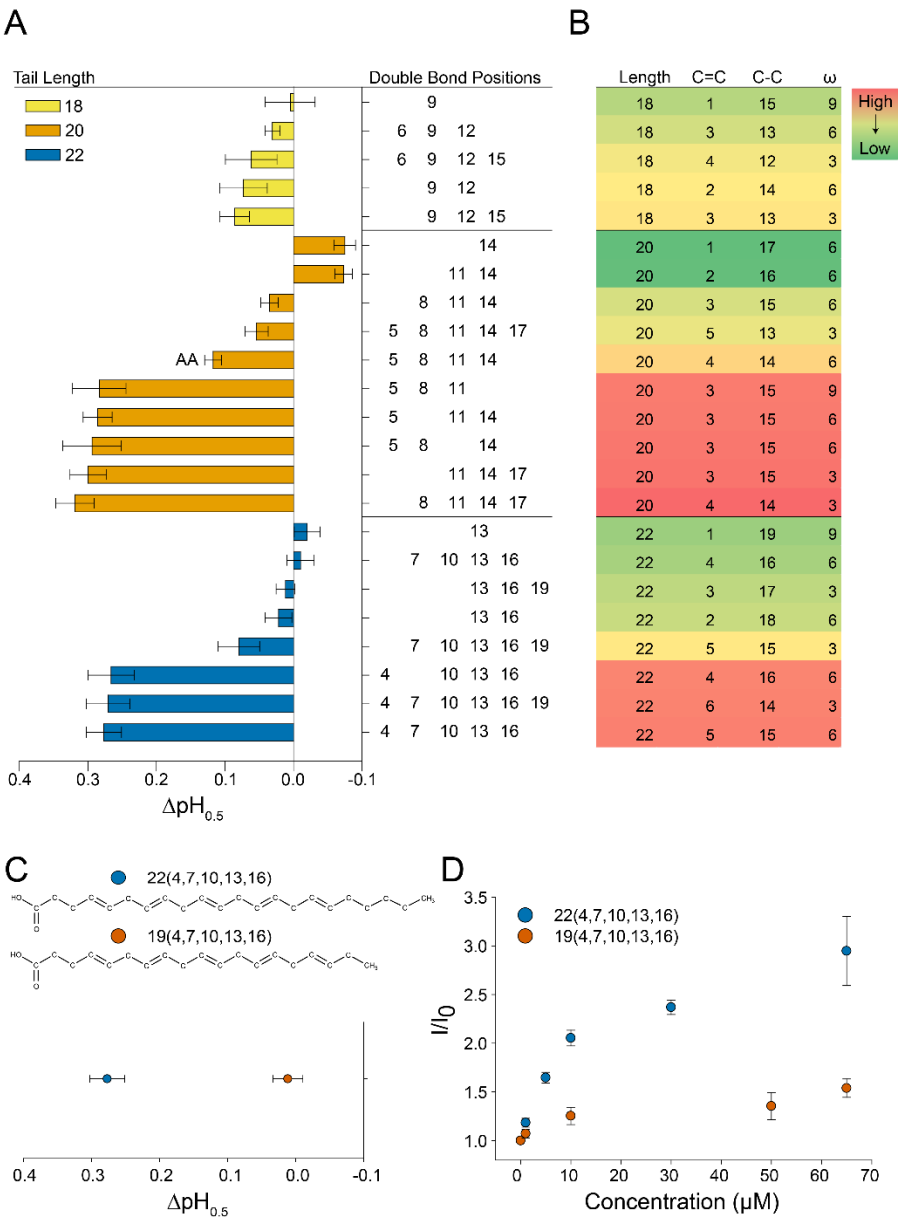

Fig. 4. Effects of PUFA tail properties on ASIC potentiation. (A) Magnitude of shifts ($\Delta pH_{0.5}$) in ASIC3 pH dependence of activation induced by 10μM of PUFAs with differing tails. Tails are grouped by tail length and then ordered based on the magnitude of their effect. The exact positions of the tail double bonds are given on the y-axis. (Data given in Table 1). (B) Heat map showing various tail properties (length, number of double bonds, number of single rotatable bonds, and ω-number) for the data in panel A. Each row in panel B corresponds to the PUFA adjacent in panel A. Dark red indicates largest alkaline $\Delta pH_{0.5}$ measured while dark green indicates a small acidic shift. (C) Structures (top) and $\Delta pH_{0.5}$ (bottom) for two PUFAs with identical double bond positions but differing acyl tail lengths ($pH_{0.5}$ = 6.83 ± 0.03, n = 5, $p < 0.0001$ for [22(4,7,10,13,16)]; and 6.57 ± 0.02, n = 6, p = 0.68 for [19(4,7,10,13,16,19)]). (D) Plot showing the fractional change in peak current for two different lipids at increasing lipid concentrations. Currents were measured from pH jumps from 8.0 to 6.6 and peak currents at each concentration were normalized to peaks in the absence of PUFA. All data given as Mean ± SEM.

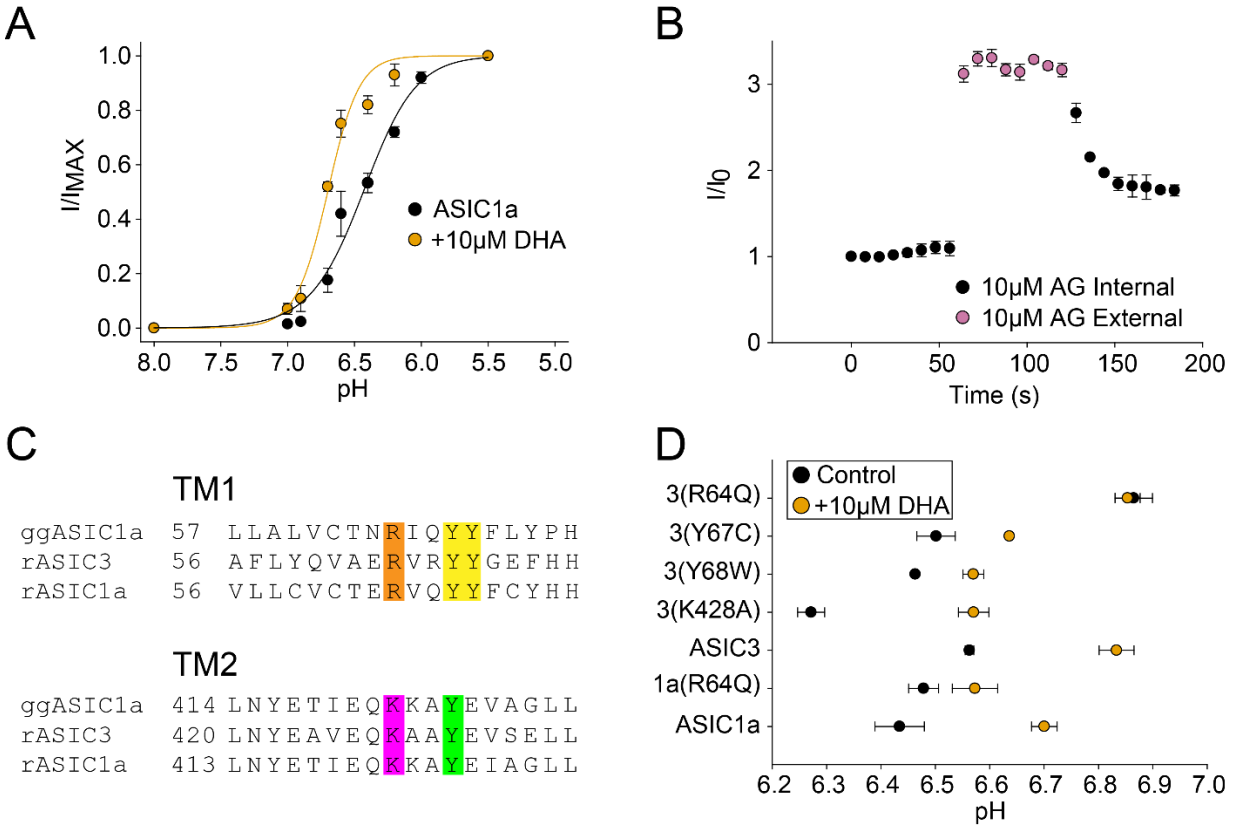

Fig. 5. PUFA potentiation of ASICs is dependent on an arginine residue in TM1. (A) pH dependence of activation of ASIC1a control and +10μM DHA ($pH_{0.5}$ = 6.43 ± 0.05, n = 7 for control; and 6.70 ± 0.02, n = 6 for ASIC1a + 10μM DHA; p = 0.002). (B) Subsequent pH 6.6 activations from a holding pH (8.0) for ASIC3 demonstrates that internal application of 10μM AG does not potentiate ASIC3 while extracellular 10μM AG produces a rapid potentiation. (C) Sequence alignment for the extracellular segments of TM1 and TM2 for chicken ASIC1a, rat ASIC1a, and rat ASIC3. Highlighted residues represent potential PUFA regulation sites. (D) $pH_{0.5}$ for ASIC mutants with and without 10μM DHA (Data given in Table 2). (E) Structure of ggASIC1a. Highlighted residues correspond to same colors in C. All mutated residues that showed diminished potentiation upon application of 10μM DHA compared to WT are found within the same "pocket" which may serve as the key interaction site for the PUFA head group. Structure visualized using Chimera 1.12 and PDB 6VTK (63). All data given as Mean ± SEM.